IEEE Access
Multidisciplinary | Rapid Review | Open Access Journal

Received 4 October 2024, accepted 4 November 2024, date of publication 7 November 2024, date of current version 25 November 2024.

Digital Object Identifier 10.1109/ACCESS.2024.3493815

RESEARCH ARTICLE

Experimental Investigation of Free Space Optical Channel Performance in the Arctic Weather

SAHIL NAZIR POTTOO[1], (Graduate Student Member, IEEE), PÅL GUNNAR ELLINGSEN[1], AND TU DAC HO[1,2], (Senior Member, IEEE)

[1]Department of Electrical Engineering, UiT The Arctic University of Norway, 8514 Narvik, Norway
[2]Department of Information Security and Communication Technology, Norwegian University of Science and Technology, 7491 Trondheim, Norway

Corresponding author: Sahil Nazir Pottoo (sahil.n.pottoo@uit.no)

This work was supported by the Grant from the Publication Fund of UiT—The Arctic University of Norway for publication charges.

ABSTRACT This paper investigates the technical aspects of the 1550 nm free space optical (FSO) link in extreme Arctic weather, specifically in falling snow, which is currently understudied. We measured the time variation of the received optical power in many snowfall events and derived attenuation statistics. Continuous measurements allowed us to estimate attenuation under varying temperatures and humidity to examine the after-snow channel impairments. Our results show several shortcomings in the International Telecommunication Union-Radio Communication (ITU-R) snow attenuation model and verify that a correlation exists between snow features, snowfall rate, temperature, and humidity in determining the total snow attenuation. We demonstrated the relationship between snow properties, temperature, humidity, and attenuation under both in-snow and post-snow environments. Furthermore, based on the experimental results, we recommend several mitigation techniques to realize FSO communication during challenging Arctic weather conditions. Lastly, we present a feasibility study of FSO in Svalbard at 78°N latitude.

INDEX TERMS Free space optical communication, optical attenuation, Arctic broadband, atmospheric measurements, channel modeling, unmanned aerial vehicles.

I. INTRODUCTION

The Arctic is undergoing rapid development due to increased shipping, tourism, research, oil, gas, and mineral extraction, which poses a significant challenge for telecommunications capabilities [1]. From 2013 to 2023, the Arctic experienced a 37 % increase in unique ships and 111 % increase in sailing distances [2]. Geostationary satellites do not provide broadband services beyond 75°N and air or maritime traffic depends on unidirectional voice links or iridium satellite phones [3]. In addition, there are insufficient polar satellites to provide continuous connectivity at the necessary bandwidth; they involve massive cost, and complicated orbit positions and maneuvers. Therefore, the present telecom infrastructure is insufficient to support the expansion of economic interest in the Arctic. A comprehensive account of the telecommunications infrastructure focused on Svalbard is presented in Section VI.

Owing to geography and dispersed population, no single technology is appropriate for all telecommunication demands in the Arctic [3]. Hence, a combined approach for adopting and deploying sustainable heterogeneous (radio/optical) and integrated (ground/sea/air/space) connectivity solutions is important. The design and deployment of non-terrestrial networks (NTNs) are recognized as priority areas for international and national telecommunications initiatives worldwide [4]. For instance, unmanned aerial vehicle (UAV) assisted cellular and broadband communications are attractive to telecom companies [5]. UAVs can overcome topographic challenges and do not require permanent terrestrial stations to establish communication links. One potential candidate for realizing multi-gigabit UAV-to-ground and ground-to-UAV communications, that is, employing UAVs as aerial base stations, is free space optical (FSO) communication [6]. FSO is similar to fiber-in-air, license-free, cyber

The associate editor coordinating the review of this manuscript and approving it for publication was Maged Abdullah Esmail.

© 2024 The Authors. This work is licensed under a Creative Commons Attribution 4.0 License.
For more information, see https://creativecommons.org/licenses/by/4.0/

attack-resistant, and low-power technology offering 5G/6G network performance. Mobile FSO systems using rotor-wing or fixed-wing UAVs can be deployed for wireless on-demand networks, disaster management, and search and rescue (SAR). A multirotor drone can operate during short service requirements, whereas a fixed-wing drone can operate for several hours at altitudes ranging from 2 km to 3 km, which is higher than rescue helicopters, thus avoiding collisions when SAR is underway [7]. To extend the service time of UAVs, several wireless charging solutions have been demonstrated using inductive or capacitive wireless power transfer in [8], [9], [10], and [11] and simultaneous lightwave information and power transfer (SLIPT) in [12] and [13]. Otherwise, tethered drones could be operated when hovering over a specific area, presented for example in [14] and [15]. UAVs and high-altitude platforms (HAPs) are far more economical to manufacture, launch, operate, and maintain than satellites, and are much more responsive. Another application is to establish ship-to-ship and ship-to-shore high-speed FSO links [16].

The major challenges for Arctic broadband systems are the extreme weather conditions for mobile wireless systems and infeasible terrain for wireline transmissions. Snow is a typical form of precipitation in the Arctic, and determining FSO attenuation in falling snow has received less attention. Khamidullin et al. [17] reported measurement of received optical power for one hour on some snow days in Kazakhstan and calculated path loss of 8.66 dB at 4.7 mm h^{-1} snowfall rate for 1550 nm laser source. Nebuloni et al. [18] propagated a 785 nm laser beam during snowfall in Italy and found that using a visibility sensor to estimate snow attenuation led to substantial underestimates because of the small sample volume. The authors in [19] reported the attenuation of visible light by falling snow using visibility and photometer measurements, in which visual inspection and mass accumulation were used to categorize snow features. However, visibility-based attenuation modelling is unreliable and visual inspection is prone to human error. Rahm et al. [20] calculated the transmission efficiencies of a 1557 nm pulsed laser source assuming spherical snow particles and Mie scattering, which are invalid for snow based on the size parameter described in Subsection II-A. The authors in [21] investigated three dry snow events at Graz and reported a peak attenuation of 68 dB km^{-1} at a wavelength of 950 nm. Nonetheless, they used a visibility-based formula to estimate the snow attenuation, which is unreliable. Akiba et al. [22] experimented in Japan with a 780 nm laser and the power level declined sharply for approximately 10 ms when snowflakes intersected the beam path. Regardless, their measurement lasted three hours and recorded only two snowfall rates obtained from a meteorological station 2 km away. Renaud and Federici [23] reported that the effects of atmospheric humidity must be included when modelling snow attenuation.

The International Telecommunication Union-Radio Communication (ITU-R) reports ITU-R F.2106-1 [24], ITU-R P.1817-1 [25], and ITU-R P.1814 [26] recommend a power-law formula for the prediction of snow attenuation. The model is based on two variables, snowfall rate and operating wavelength, and two pre-calculated coefficients. Different locations on Earth may record the same snowfall rate and have FSO systems operating at the same wavelengths, leading the ITU-R model to predict identical attenuation. This is improbable owing to variations in snow formation factors, snowflake properties, laser beam diameter, and snow distribution in the atmosphere. These parameters are not accounted for in the ITU-R model. Among all weather elements, it is most difficult to determine attenuation from snow due to the complex and unique snow features, further explained in Subsection II-A.

Therefore, motivated by fewer studies, uncertainties, and challenges of modelling FSO attenuation in snow, to the best of our knowledge, for the first time, we have reported day/night field measurements of the received laser power in snowfall in the Arctic region. We also compared the calculated snow attenuation with the ITU-R wet snow and dry snow models under the coupled effects of temperature and humidity. Furthermore, we analyzed the post-snow received signal strength and attenuation caused by the temperature and humidity. We demonstrated the relationship between temperature and humidity and described how water vapor-induced attenuation increased with the evaporation of ground snow.

The remainder of this paper is organized as follows. Section II provides a theoretical overview of the laser-snow interaction and the ITU-R model. Section III presents the measurement setup. Section IV describes the experimental results. In Section V, we recommend snow attenuation mitigation techniques. Section VI explains the coverage gaps and feasibility of FSO in Svalbard. Concluding remarks are presented in Section VII.

II. THEORETICAL ANALYSIS

Several factors characterize the type, size, shape, and distribution of snowflakes in the atmosphere. Furthermore, in falling snow, these features change within minutes, and hence, are difficult to predict and document. Therefore, in the following subsections, we analyze the laser-snow interaction and limitations of the ITU-R model.

A. INTERACTION BETWEEN LASER BEAM AND SNOWFLAKES

The formation of snow requires two specific weather conditions: low temperature and high humidity in the air, which ultimately determine the properties of the snowflakes [27] and consequently the snow attenuation level. Snowflakes possess complex and unique shapes and are primarily non-spherical crystals. Temperatures at or above 0 °C produce wet snow whereas temperatures below 0 °C produce dry snow. One characteristic of wet snow is that it contains a liquid coating. This coating implies that the flakes easily fuse to form larger and denser snow aggregates [28]; thus, wet

snow may cause high optical attenuation. Dry snow has no surrounding liquid, which gives the dry flakes a powdery texture. The laser beam re-emerges from a snowflake by surface reflection and refraction from the internal snow structures. Some photons are absorbed, whereas the emitted photons exhibit directional changes at each air-snow periphery. Snow crystals are known to have strong absorption in the near-infrared (NIR) band [29], resulting in lower snow albedo (aka reflectance) at 1550 nm. The scattering effect depends on the size parameter $x = 2\pi r/\lambda$ where λ is the wavelength and r is the snowflake radius, and if $x \geq 2000$, geometric scattering occurs [30]. Considering $\lambda = 1550$ nm and $r = 0.5$ mm (smaller flake), we obtain $x = 2025$ which implies that snow causes geometric scattering of the laser beam. This causes beam deflection, roll, and decentering motion. When laser light scatters from snow aggregates along the beam path, it induces beam wandering.

B. SNOW ATTENUATION

Currently, no reliable model exists for the precise estimation of laser attenuation caused by falling snow. The ITU-R recommended power law converts the snowfall rate into the specific attenuation, but there is no unambiguous evidence of its accuracy. The ITU-R snow attenuation model is [24], [25], [26]

$$\gamma_s = a(R_s)^b \tag{1}$$

where γ_s is the predicted snow attenuation in dB km^{-1}, R_s is the liquid water equivalent or snowfall rate in mm h^{-1}, a and b are empirical coefficients, and for wet snow and dry snow are expressed as

$$a_{\text{wet snow}} = (0.0001023)\lambda + 3.79, \; b_{\text{wet snow}} = 0.72 \tag{2}$$
$$a_{\text{dry snow}} = (0.0000542)\lambda + 5.50, \; b_{\text{dry snow}} = 1.38 \tag{3}$$

Solving Eqs. (2) and (3) for 1550 nm and substituting them into Eq. (1), the snow attenuation models are:

$$\gamma_{\text{wet snow}} = 3.95(R_s)^{0.72} \tag{4}$$
$$\gamma_{\text{dry snow}} = 5.58(R_s)^{1.38} \tag{5}$$

This specific attenuation model may not be applicable globally across various snowfall conditions and geographical regions. Although ITU-R has published new recommendations over time, the snow attenuation model has remained unmodified. It is noteworthy that Eqs. (10) and (11) in [24] are identical to Eq. (7) and Table (3) in [26], but the latter does not specify that different altitudes delimit wet and dry snow. Furthermore, the model does not consider local weather and geometrical scattering, which instigate physical changes in snow and distortions in the laser beam, as described in Subsection II-A. Hence, a deeper understanding of laser snow attenuation theory and experiments at diverse locations are required to derive accurate snow attenuation statistics for the FSO link.

III. EXPERIMENT SETUP

Our experiment was conducted at UiT The Arctic University of Norway in Narvik, from March to May 2023. The FSO link was established 4 m above the roof, 12 m above the ground, and 105 m above the sea level. The setup for the outdoor measurement is shown in Fig. 1. Real-time weather data were obtained from the Narvik Centre meteorological station (ID SN84701) operated by The Norwegian Meteorological Institute [31], located 600 m from the experimental site. The small form-factor FSO system was built using off-the-shelf components. It consists of a transmitter and receiver with dimensions of 7 × 20 × 10 cm and 10 × 20 × 10 cm, respectively. Table 1 presents the specifications of the FSO link. An InGaAsP laser diode (Thorlabs ML925B45F) fitted inside a strain-relief cable (Thorlabs SR9D) was operated using a constant-current laser driver (Thorlabs LD1255R). The laser output was a stable continuous wave of 5 mW optical power at a center wavelength of 1550 nm. A collimated beam was produced using an aspheric lens (Thorlabs 354330-C), and beam steering was performed using two broadband mirrors (Thorlabs BB1-E04). At the receiver, a planoconvex lens (Thorlabs LA1131-C) focused the incoming laser beam onto a germanium photodiode power sensor (Thorlabs S122C) connected to a power meter (Thorlabs PM100D). The received laser power was logged at a temporal resolution of 300 ms. Both setups were securely fastened and placed inside weatherproof acrylate boxes with narrow holes for the beam exit and entry. The laser alignment was performed manually at the start of the experiment. No realignment was performed during the experiment.

TABLE 1. FSO system specifications.

Parameters	Specification
Transmitter laser power	5 mW
Optical wavelength	1550 nm
Transmitting lens focal length	3.1 mm
Beam divergence	0.494 mrad
Range	20 m
Receiving lens focal length	50 mm
Receiving lens diameter	25.4 mm
Detector response time	< 1 µs
Detector active area	9.7 mm x 9.7 mm
Detector input aperture	9.5 mm
Detector responsivity	0.07 A/W
Detector measurement uncertainty	± 5 %

IV. RESULTS AND DISCUSSION

In the subsequent subsections, we present our findings and discuss the effects of typical Arctic weather conditions on FSO transmission performance using measurement statistics. In addition to the snowfall rate versus received power and attenuation, we show the interrelationship between snowfall rate, temperature, and humidity in determining snow attenuation. We also measured the received optical power and calculated the attenuation under temperature, humidity, and no precipitation conditions to investigate the after-snow channel effects. Attenuation was computed as the difference

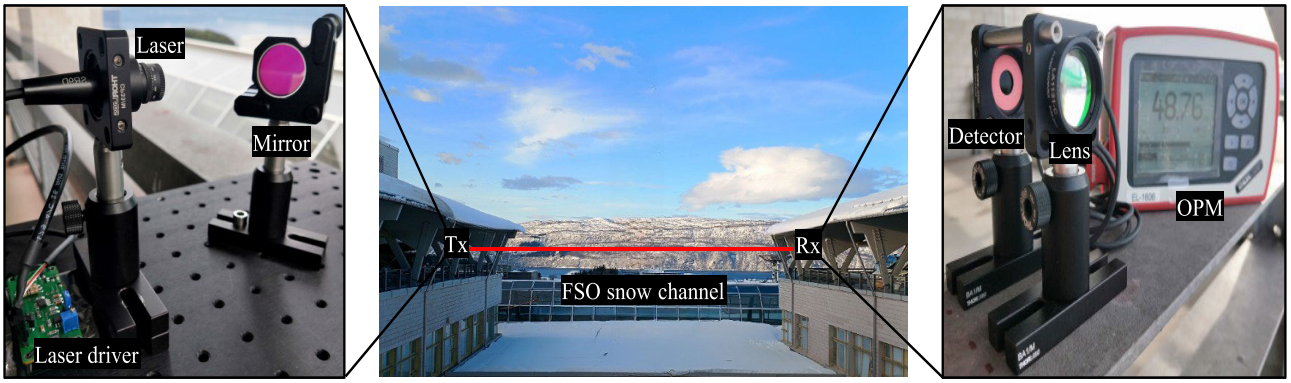

FIGURE 1. Outdoor FSO measurement setup showing transmitter (Tx) and receiver (Rx) with an optical power meter (OPM).

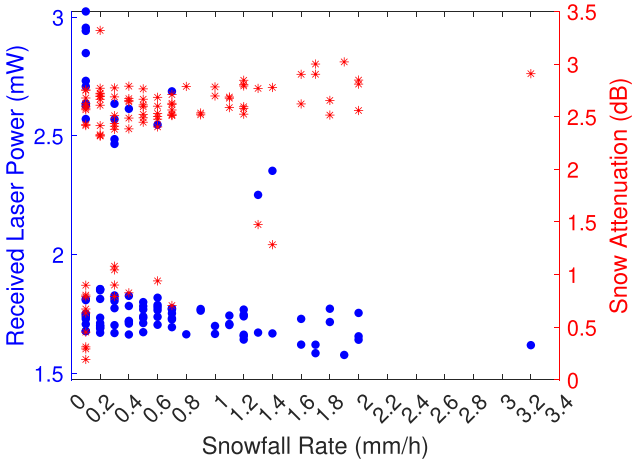

FIGURE 2. Received laser power and attenuation under snow events (no rain).

between the maximum system received power (3.1 mW) and instantaneous received power. Excess attenuation was caused by snow in the respective snow periods and water vapor at other times. Temperature and humidity have a continuous influence on both falling snow and accumulated snow. On numerous other days, the received power was measured to be approximately 3.1 mW which confirms that the FSO system can reach the maximum value under appropriate conditions.

A. RECEIVED OPTICAL POWER AND ATTENUATION UNDER SNOWFALL

The received laser power and attenuation against the snowfall rate are shown in Fig. 2. Table 2 describes the weather conditions during data acquisition in snowfall events. The same snowfall rate has produced a range of attenuation, for instance at 0.1 mm h^{-1}, attenuation fluctuated between 0.19 dB to 2.75 dB and so forth. The distribution of attenuation at a constant snowfall rate indicates the combined effects of local weather and snow features, which supports the discussion in Subsection II-A. Note that high attenuation is obtained at both low and high snowfall rates. A rate of

TABLE 2. Snow events recorded in the measurement period March to May 2023.

Date	Snowfall period (CET)	Snow water equivalent (mm)	Average temperature (°C)	Average humidity (%)
2023-03-21	08–18	1.4	-0.9	77
2023-03-30	08–12, 22–23	2.7	-2.6	90
2023-04-01	03–09, 12–13	2.7	-0.4	87
2023-04-21	07–24	10.8	4.6	89
2023-04-22	00–2, 11–16	1.8	-0.2	83
2023-04-28	03–24	17.3	2.7	95
2023-04-29	00–24	14.5	1.1	94
2023-04-30	00–07	7.4	0.8	95
2023-05-02	00–12, 17–18	6.6	2.3	87

0.2 mm h^{-1} caused 3.32 dB attenuation while 3.2 mm h^{-1} produced 2.91 dB attenuation. The high attenuation at low snowfall rates could be explained by larger snowflakes across the beam path, blocking more of the laser beam and high humidity. This result reveals that snowfall rate is not a single main factor driving laser attenuation in snowfall. Rather it is a function of snow features (rate, type, size, distribution) and environmental conditions through snow events and these elements cannot be neglected.

In Fig. 3, we demonstrate the coupling effect of snowfall rate, temperature, and humidity on attenuation. The calculated attenuation up to 1 km was compared with that in Eqs. (4) and (5) of the ITU-R wet snow and dry snow models. Temperatures below or above 0 °C also indicate the presence of dry snow or wet snow events during the measurements. The results showed that the ITU-R models underestimated the attenuation to a large extent. When the snowfall rate was constant and the temperature and humidity varied, the snow characteristics changed, causing attenuation fluctuations. Snow attenuation of 100 dB km^{-1} to 150 dB km^{-1} was found for humidity of 90 % to 100 % and temperatures of 0 °C to 3 °C. Continuous variations in humidity and temperature contributed to snow attenuation because they changed the snow type and size within minutes

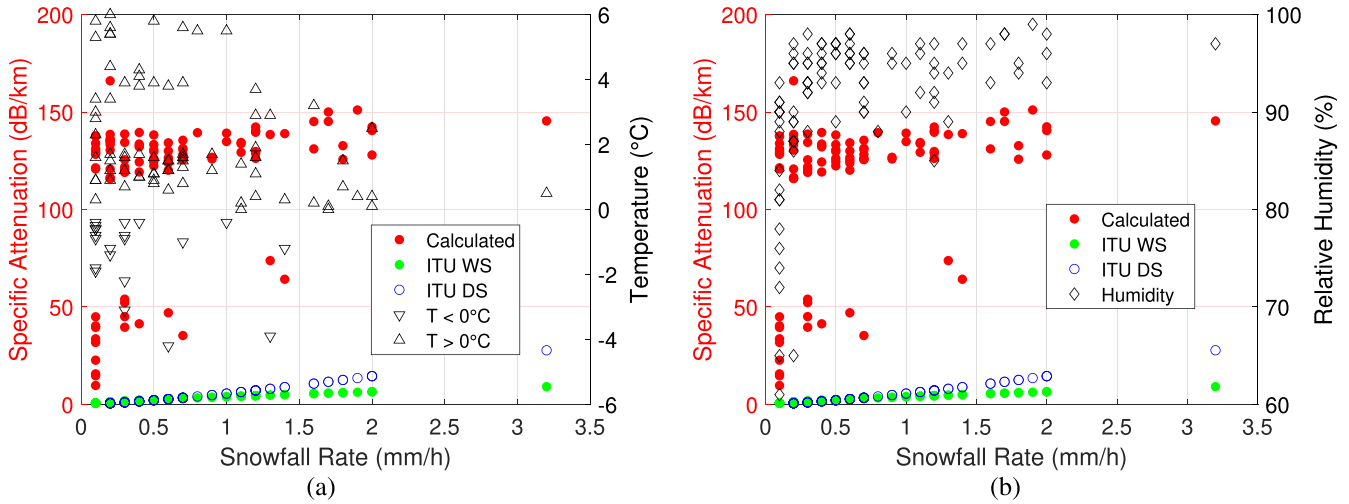

FIGURE 3. Estimated snow attenuation compared to ITU wet snow (WS) and dry snow (DS) models under snow determining factors (a) air temperatures during snowfall and (b) relative humidity during snowfall.

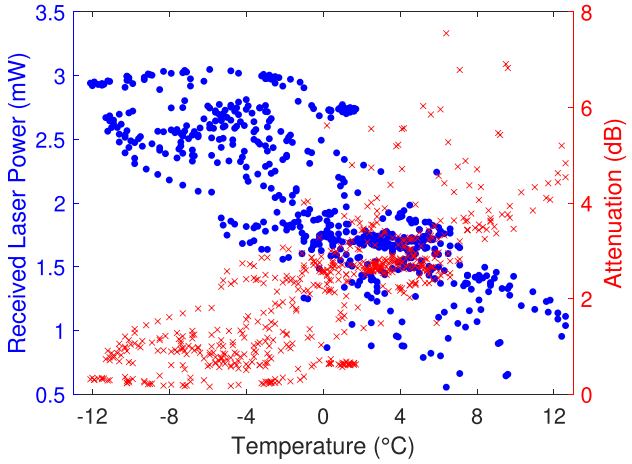

FIGURE 4. Received laser power and attenuation under varying temperatures (no snow/rain). Based on measurements between 2023-03-21 and 2023-05-10.

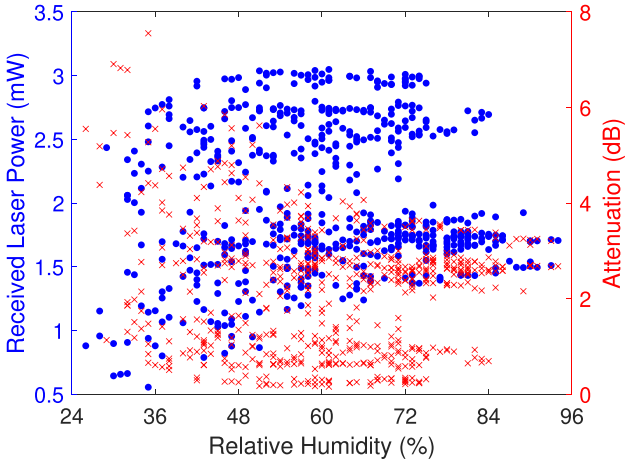

FIGURE 5. Received laser power and attenuation under varying humidity (no snow/rain). Based on measurements between 2023-03-21 and 2023-05-10.

and the water vapor content in the air. Hence, from these results and statistics, we deduce that during a snow event if the temperature is above 0 ° C and the relative humidity is very high, the attenuation increases; otherwise, it is less.

B. RECEIVED OPTICAL POWER AND ATTENUATION UNDER TEMPERATURE AND HUMIDITY

The measured received power and attenuation profiles with changing temperatures in the absence of precipitation from 2023-03-21 to 2023-05-10 are shown in Fig. 4. The distribution of attenuation with temperature has a clear trend, where warmer temperatures cause high attenuation, and freezing temperatures cause low attenuation. One reason is that the humidity increases at higher temperatures due to evaporation from the melting ground snow. A linear relationship is found between temperature and attenuation. The received laser power and optical attenuation with respect to the humidity are shown in Fig. 5. The scatter plot shows a dispersed relationship between humidity, power, and attenuation in the absence of rain and snow. In reality, a complex interplay exists between temperature, humidity, and air pressure, which alter the atmosphere within the link range. From these measurements, it can be established that regions where snowfall is frequent, with the continuous presence of accumulated snow and subsequent melting and evaporation processes, can undergo higher attenuation in the absence of precipitation. This condition is illustrated in Fig. 7d. This highlights the need to mitigate post-snowfall channel impairments to ensure optimal link availability.

The humidity distribution over the temperature range, including snow events, is shown in Fig. 6. This result elucidates the relationship between humidity and temperature, and its significant impact on the water vapor concentration of air in snow regions. This clarifies why high attenuation was obtained for temperatures above 0 ° C. Hence, excess water

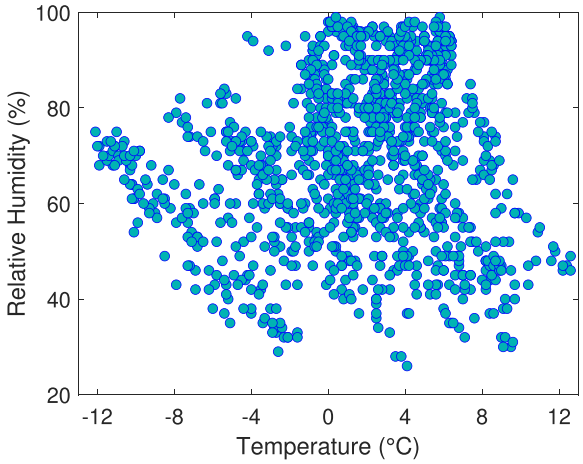

FIGURE 6. Relation between relative humidity and temperature in the Arctic region. Based on measurements between 2023-03-21 and 2023-05-10.

vapor in the air in snowy regions influences both in-snow and post-snow attenuation.

C. MEASUREMENT UNCERTAINTIES

We have been very careful with data processing from measurements, meteorological data, and visual observations to separate snow and rain events; therefore, there is no merger between them in our results. However, the occurrence of mixed rain and snow cannot be completely dismissed. It is challenging to comprehend the rapid phenomena occurring in the atmosphere, in particular, the Arctic environment is difficult to model. There is also 24 × 7 turbulence, scintillation, beam wander, and scattering affecting free space laser propagation. We found the exact timings of snow events and the excess attenuation in those periods was caused by snow only. Otherwise, when precipitation was zero we consider that was clear air attenuation, at our experiment site primarily due to the high evaporation rate of ground snow which increased water vapor-induced attenuation with rising temperatures. In addition, wind affects the distribution of falling snow in the air. The fog was absent during the measurements and the average visibility was 10 km.

V. MITIGATION OF SNOW ATTENUATION

After we have established the degradation of FSO link in falling snow and post-snow environments, the implementation of a snow-resistant and self-healing FSO system is necessary. Therefore, we recommend mitigation solutions for snow attenuation taking into account our measurement results and observations. These are discussed as follows.

1) Beam width optimization: Larger snowflakes can completely block the optical signal if the beam width is smaller than its size. To mitigate the beam wandering and obstruction caused by the flake size distribution, the transmitted beam diameter should be increased. In our FSO setup, the beam diameter was 2.82 mm at the transmitter, and owing to divergence it was 12.7 mm at the receiver. By employing a beam expander, a larger beam diameter and smaller divergence angle are possible, which reduces the possibility of partial or full beam blockage by distinct snowflake sizes. The authors in [22] found that the bit error rate performance could be improved by increasing the transmitted beam size under snow conditions.
2) Coherent FSO system: A coherent FSO system using economical small form-factor pluggable (SFP/SFP+) optical transceivers to improve FSO transmission resilience in the snowy atmosphere is shown in Fig. 7a. Coherent technology is more robust against atmospheric degradation than traditional intensity modulation and direct detection. To fully leverage this advantage, the transponder should be redesigned for snow channel characteristics. High-capacity coherent pluggables and fiber/FSO coupling would also enable seamless wavelength-division multiplexed transmission.
3) Multiple transmitter and diversity combining techniques: These two schemes are illustrated in Fig. 7b. An array of compact FSO transmitters reduces the probability that multiple laser beams pass through identical snow distributions. Thus, the likelihood of simultaneous signal degradation across all channels is reduced by the spatial arrangement and diverse snow distribution caused by wind. In our work, a single-channel FSO system was implemented, which would not be very effective under long periods of heavy snowfall and uniform snow concentration in the air, unless the beam was made unreasonably large, which would also decrease the power density. On the receiver side, diversity-combining techniques would optimally combine multiple independent beams to improve detection efficiency and combat fading [32].
4) Aperture averaging: A larger aperture size or active area of the detector captures more laser power and averages out the effects of fading and beam wander, thereby reducing power fluctuations in snow conditions. This is shown in Fig. 7c.
5) Automatic power control (APC): Automatic transmission power control to offset rapid snow feature transitions can help maintain link availability. APC involves modifying the power gain of an erbium-doped fiber amplifier depending on the received signal strength indication [33]. This power-on-go adjustment has been depicted by varying colour intensity of the beam in Fig. 7c. The APC can stabilize the received power to combat both in-snow and post-snow channel impairments.
6) Elevated FSO installation: Installing FSO systems at higher positions above the ground is critical in snowy regions. As shown by our results, the evaporation of melting ground snow and rain would significantly increase the water vapor concentration in the atmosphere, further increasing the attenuation. This

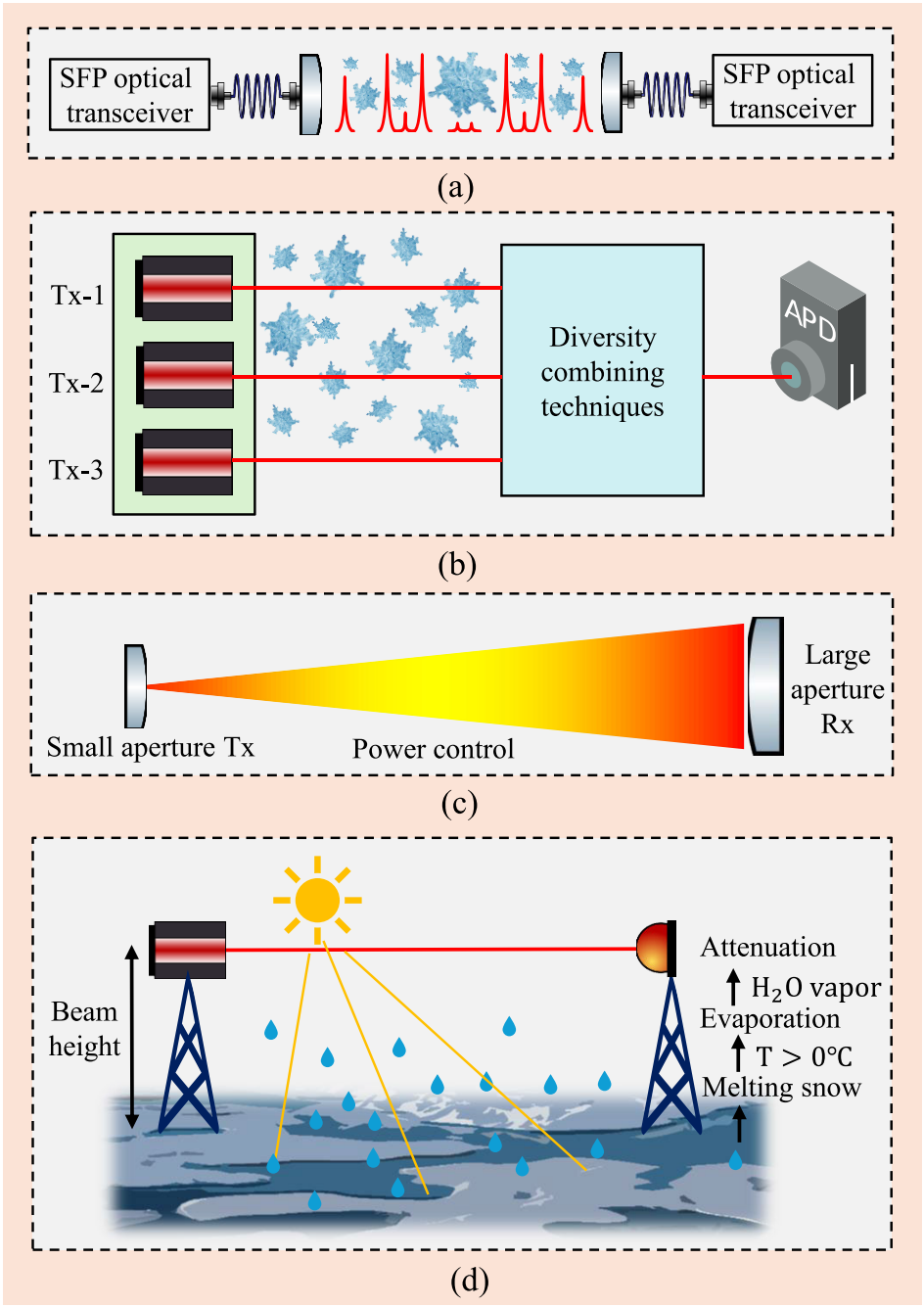

FIGURE 7. Illustration of various snow attenuation mitigation techniques (a) coherent FSO transmission, (b) multiple transmitter and diversity combining techniques, (c) aperture averaging and automatic power control, and (d) elevated installation.

situation is illustrated in Fig. 7d. A high beam height reduces the interaction of the laser beam with moisture layers and turbulence cells near the ground. UAV-mounted vertical FSO links have an innate immunity to near-ground beam degradation.

Passive mitigation techniques, namely aperture averaging, optimized beam waist, and elevated installation, must be incorporated into every FSO system functioning in snowy regions. Passive techniques offer simple solutions, easy implementations, and effective performances. Furthermore, one of the active compensation techniques such as coherent design, APC, transmit diversity, and diversity combining schemes should be employed to enhance the self-healing capabilities of the FSO links. The joint implementation of multiple transmitters and diversity combining techniques is a wise alternative. Nevertheless, active compensation methods are hardware-intensive, leading to complex design, and may involve advanced digital signal processing.

VI. FEASIBILITY STUDY OF FSO IN SVALBARD AT 78°N

This section analyzes the feasibility of deploying FSO communication systems in Svalbard. We reviewed Svalbard weather conditions and identified weaknesses in the telecom infrastructure that FSO could replenish.

Nevertheless, weather is a natural barrier for any Arctic communication system, and likewise for the FSO. The mean annual precipitation measured in the Longyearbyen area is approximately 200 mm, which is lower than the driest areas in the Norwegian mainland and less than half of the values measured at Ny-Ålesund. Daily precipitation exceeding 1 mm averages 50 days annually and exceeds 5 mm eight days annually. The number of days with snow cover has decreased since the 1970s and will continue to decline according to climate models [34]. The Norwegian Defense Research Institute (FFI) investigated cloud cover over the Arctic to estimate the feasible location of an optical ground station (OGS) for laser satellite communications [35]. They found that the maximum time percentage for cloud-free conditions was 59 % at coordinates 80.4°N 58.8°E. Two-station diversity of Platåberget in Svalbard and Bardufoss, which is near our experimental site, produced the best result with the availability of 66 %. The optical access time of polar satellites is a combination of the time above the horizon and not obscured by clouds, whereas UAVs do not have such limitations. OGS site diversity and preferably radio frequency (RF) backup are expected to improve the continuous access to satellites in the High North. The Svalbard laser ranging station may be modified to work as an OGS, enabling FSO communications with UAVs, HAPs, and polar satellites. In research stations at Ny-Ålesund on Svalbard, sensitive measurement equipment must not be exposed to RF interference, in this circumstance, FSO can provide wireless connectivity in RF-sensitive areas since electromagnetic interference does not affect laser light. Kongsberg satellite services (KSAT) operates the Svalbard satellite ground station to download data from polar-orbiting satellites, which can be transmitted to the mainland via long-distance FSO links incorporating UAV relays or HAPs.

Table 3 summarizes the milestones of telecom infrastructure development in Svalbard, which we discuss as follows. The existing telecom infrastructure in Svalbard includes Svalbard undersea twin optical fiber cables operated by Space Norway, cellular technology and fiber to homes in Longyearbyen provided by Telenor Svalbard. Figure 8 depicts the Telenor coverage map of the Svalbard islands which shows that the available mobile networks are 2G, 4G, and 4G+. The 5G network is not yet available. The 3G network was shut down in 2021. The map shows 2G covers most of the area; however, recently Telenor switched off the 2G network. 4G covers some areas while 4G+ is concentrated around Longyearbyen only. Although the residents of Ny-Ålesund can now connect to 4G network, WiFi and Bluetooth are still prohibited to prevent RF interference with scientific equipment [36]. Hence, wireless connectivity must be extended to support wider regions,

TABLE 3. Timeline of important telecom developments in Svalbard.

Year	Event
1911	Spitsbergen radio was built and started operation
1950	Local radio station operated in Longyearbyen
1978	Satellite connection in commercial operation
1981	Svalbard connected to the Norwegian remote voting network
1984	Direct broadcasts of Norwegian broadcasting corporation (NRK) TV to Longyearbyen
1991	The first ISDN subscribers were connected to the digital exchange in Longyearbyen
1996	GSM mobile coverage in Longyearbyen
1998	Internet node was put into operation in Longyearbyen
2004	Svalbard undersea optical fiber became operational
2009	Telenor offered fibre to the home (FTTH) in Longyearbyen
2011	4G/LTE test network opened
2015	Telenor's Thor 7 satellite was launched and operated
2023	Ny-Ålesund received mobile network
2024	The polar satellites ASBM-1 and ASBM-2 launched on 2024-08-11

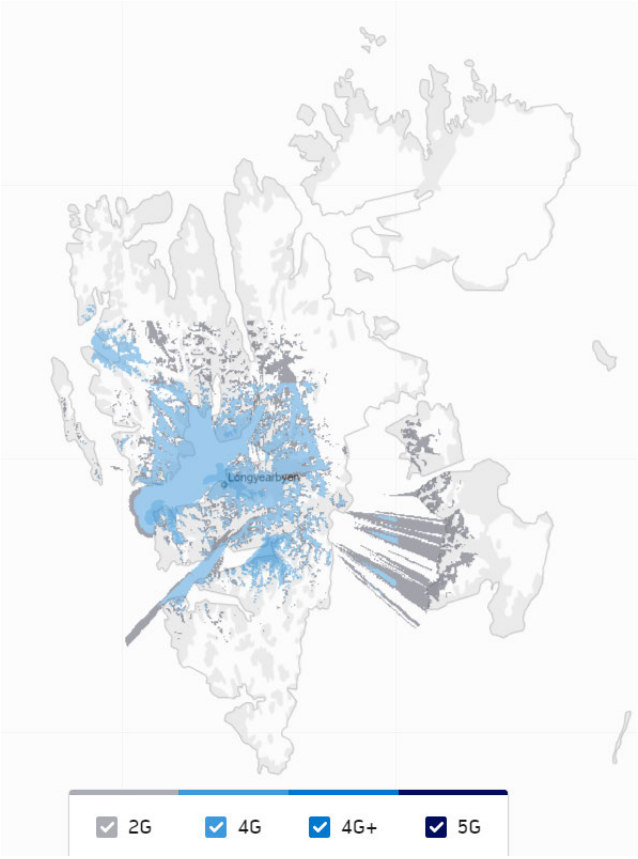

FIGURE 8. Coverage map of Svalbard archipelago from Telenor [38].

increasing activities, and local businesses, and offering an alternative to vulnerable undersea fiber cables. Recently, Starlink has started offering coverage in Svalbard although its availability and throughput remain uncertain. Under the Arctic satellite broadband mission, two polar satellites were launched on 2024-08-13 to extend broadband coverage above 65°N [37]. Each satellite can provide coverage for ten hours per period. Aerial platforms will play a crucial role in achieving full integration of satellites and terrestrial networks. NTNs operating on FSO would provide Arctic

telecommunication networks with ubiquitous connectivity, resilience, and high security.

The purpose of this feasibility study was to show that snowfall occurrence is lower in Svalbard than in the Norwegian mainland or our experimental site, Narvik. Clear air attenuation may be lower on Svalbard because the ground is permafrost, the sun is not present the entire time, and humidity and temperature variations are not large. Moreover, our results have shown that FSO performance is better at freezing temperatures, which is typical in Svalbard. The OGS site survey conducted by FFI indicates that there may be an interest and vision to establish OGS in the Arctic in the future. The coverage gap further explains the requirement of accessible broadband for an interconnected Arctic. This study assisted in unraveling opportunities for FSO in Svalbard. One solution is to employ flying fixed-wing UAV base stations operating over FSO or hybrid RF/FSO links. Therefore, increased activities towards global broadband connectivity and laser communications may drive the installation of terrestrial or aerial FSO links in the Arctic to meet the evolving needs of various sectors such as telecom, SAR, maritime, and defense.

VII. CONCLUSION

We measured the received optical power and calculated the attenuation in different snowfall events, analyzed under varying snowfall rates, temperatures and humidity profiles. The key finding of this work was to highlight and provide insights into how the temperature and humidity that determine snow features significantly contribute to total snow attenuation. We found $100\,\mathrm{dB\,km^{-1}}$ to $150\,\mathrm{dB\,km^{-1}}$ attenuation at $0.1\,\mathrm{mm\,h^{-1}}$ to $3.2\,\mathrm{mm\,h^{-1}}$ snowfall rates, $0\,^{\circ}\mathrm{C}$ to $3\,^{\circ}\mathrm{C}$ temperatures, and 90 % to 100 % humidity. In addition, unlike the conventional belief that dry snow always causes high attenuation, our results verified if the temperature is above $0\,^{\circ}\mathrm{C}$ and the relative humidity above 90 %, snow attenuation is increased. This revealed that wet snow caused high attenuation. The comparison between our results and the ITU-R model found that it underestimated attenuation to a large extent, mainly because it ignored the influence of snow-making weather parameters on attenuation. Based on the temperature and humidity results under no precipitation, we demonstrated how the evaporation of ground snow, positive temperatures, and high water vapor caused higher laser attenuation. This means that we should expect high attenuation in clear weather at the locations with the continuous presence of accumulated snow and high humidity. This study will serve as a roadmap for the design and deployment of FSO links in the Arctic to bridge the coverage gap. Further experimental research is needed at longer FSO distances with recommended mitigation techniques, preferably in Svalbard.

ACKNOWLEDGMENT

The authors thank Alexander Pankratov for making acrylate boxes by 3D laser cutting in the Energy Laboratory and Madhu Koirala for his help with manual laser beam pointing and alignment at UiT Campus Narvik.

REFERENCES

[1] Arctic Council Task Force on Telecommunications Infrastructure in the Arctic. (2017). *Telecommunications Infrastructure in the Arctic; A Circumpolar Assessment*. [Online]. Available: http://hdl.handle.net/11374/1924

[2] Protection of the Arctic Marine Environment (PAME). (2024). *The Increase in Arctic Shipping: 2013–2023*. [Online]. Available: https://hdl.handle.net/11374/2733.3

[3] Arctic Economic Council. (2017). *Arctic Broadband: Recommendations for an Interconnected Arctic*. [Online]. Available: https://arcticeconomiccouncil.com/reports/https-arcticeconomiccouncil-com-wp-content-uploads-2019-10-aec-report_final-lr-pdf/

[4] European Space Agency Connectivity and Secure Communications. *The Non-Terrestrial Networks (NTN) Forum*. Accessed: Sep. 26, 2024. [Online]. Available: https://connectivity.esa.int/nonterrestrial-networks-ntn-forum

[5] M. Matracia, M. A. Kishk, and M.-S. Alouini, "Aerial base stations for global connectivity: Is it a feasible and reliable solution?" *IEEE Veh. Technol. Mag.*, vol. 18, no. 4, pp. 94–101, Dec. 2023, doi: 10.1109/MVT.2023.3301228.

[6] C. Álvarez-Roa, M. Álvarez-Roa, F. J. Martín-Vega, M. Castillo-Vázquez, T. Raddo, and A. Jurado-Navas, "Performance analysis of a vertical FSO link with energy harvesting strategy," *Sensors*, vol. 22, no. 15, p. 5684, Jul. 2022, doi: 10.3390/s22155684.

[7] Telenor Norway. *Norwegian Technology Improves Emergency Preparedness in Svalbard*. [Online]. Available: Accessed: May 10, 2024. [Online]. Available: https://www.telenor.no/om/presse-og-media/pressemeldinger/norwegian-technology-improves-emergency-preparedness-in-svalbard.jsp

[8] J. M. Arteaga, S. Aldhaher, G. Kkelis, C. Kwan, D. C. Yates, and P. D. Mitcheson, "Dynamic capabilities of multi-MHz inductive power transfer systems demonstrated with batteryless drones," *IEEE Trans. Power Electron.*, vol. 34, no. 6, pp. 5093–5104, Jun. 2019, doi: 10.1109/TPEL.2018.2871188.

[9] Y. Shao, N. Kang, H. Zhang, R. Ma, M. Liu, and C. Ma, "A lightweight and robust drone MHz WPT system via novel coil design and impedance matching," *IEEE Trans. Ind. Appl.*, vol. 59, no. 3, pp. 3851–3864, May/Jun. 2023, doi: 10.1109/TIA.2023.3249146.

[10] C. Park, J. Park, Y. Shin, J. Kim, S. Huh, D. Kim, S. Park, and S. Ahn, "Separated circular capacitive coupler for reducing cross-coupling capacitance in drone wireless power transfer system," *IEEE Trans. Microw. Theory Techn.*, vol. 68, no. 9, pp. 3978–3985, Sep. 2020, doi: 10.1109/TMTT.2020.2989118.

[11] T. M. Mostafa, A. Muharam, and R. Hattori, "Wireless battery charging system for drones via capacitive power transfer," in *Proc. IEEE PELS Workshop Emerg. Technol., Wireless Power Transf. (WoW)*, May 2017, pp. 1–6, doi: 10.1109/WOW.2017.7959357.

[12] M.-A. Lahmeri, M. A. Kishk, and M.-S. Alouini, "Laser-powered UAVs for wireless communication coverage: A large-scale deployment strategy," *IEEE Trans. Wireless Commun.*, vol. 22, no. 1, pp. 518–533, Jan. 2023, doi: 10.1109/TWC.2022.3195867.

[13] M.-A. Lahmeri, M. A. Kishk, and M.-S. Alouini, "Charging techniques for UAV-assisted data collection: Is laser power beaming the answer?" *IEEE Commun. Mag.*, vol. 60, no. 5, pp. 50–56, May 2022, doi: 10.1109/MCOM.001.2100871.

[14] M. Kishk, A. Bader, and M.-S. Alouini, "Aerial base station deployment in 6G cellular networks using tethered drones: The mobility and endurance tradeoff," *IEEE Veh. Technol. Mag.*, vol. 15, no. 4, pp. 103–111, Dec. 2020, doi: 10.1109/MVT.2020.3017885.

[15] S. Khemiri, M. A. Kishk, and M.-S. Alouini, "Coverage analysis of tethered UAV-assisted large-scale cellular networks," *IEEE Trans. Aerosp. Electron. Syst.*, vol. 59, no. 6, pp. 7890–7907, Dec. 2023, doi: 10.1109/TAES.2023.3300296.

[16] A. Willitsford, K. T. Newell, M. O'Toole, and K. Patel, "Maritime free space optical communications field test and link budget statistics," *Opt. Exp.*, vol. 32, no. 8, pp. 13769–13782, Apr. 2024, doi: 10.1364/oe.518363.

[17] A. Khamidullin, R. C. Kizilirmak, M. Uysal, and I. A. Ukaegbu, "FSO link attenuation measurement in extreme winter conditions for secure 5G applications," *Proc. SPIE*, vol. 12427, Mar. 2023, Art. no. 124270C, doi: 10.1117/12.2648075.

[18] R. Nebuloni and C. Capsoni, "Laser attenuation by falling snow," in *Proc. 6th Int. Symp. Commun. Syst., Netw. Digit. Signal Process.*, Jul. 2008, pp. 265–269, doi: 10.1109/csndsp.2008.4610768.
[19] H. W. O'Brien, "Visibility and light attenuation in falling snow," *J. Appl. Meteorol. Climatol.*, vol. 9, no. 4, pp. 671–683, 1970, doi: 10.1175/1520-0450(1970)009<0671:VALAIF>2.0.CO;2.
[20] M. Rahm, P. Jonsson, and M. Henriksson, "Laser attenuation in falling snow correlated with measurements of snow particle size distribution," *Opt. Eng.*, vol. 60, no. 9, Sep. 2021, Art. no. 094102, doi: 10.1117/1.oe.60.9.094102.
[21] M. S. Awan, L. C. Horwath, S. S. Muhammad, E. Leitgeb, F. Nadeem, and M. S. Khan, "Characterization of fog and snow attenuations for free-space optical propagation," *J. Commun.*, vol. 4, no. 8, pp. 533–545, Sep. 2009, doi: 10.4304/jcm.4.8.533-545.
[22] M. Akiba, K. Ogawa, K. Wakamori, K. Kodate, and S. Ito, "Measurement and simulation of the effect of snowfall on free-space optical propagation," *Appl. Opt.*, vol. 47, no. 31, pp. 5736–5743, Nov. 2008, doi: 10.1364/ao.47.005736.
[23] D. L. Renaud and J. F. Federici, "Terahertz attenuation in snow and sleet," *J. Infr., Millim., Terahertz Waves*, vol. 40, no. 8, pp. 868–877, Aug. 2019, doi: 10.1007/s10762-019-00607-y.
[24] International Telecommunication Union Radio Communication. (2010). *Fixed Service Applications Using Free-Space Optical Links*. [Online]. Available: https://www.itu.int/dms_pub/itu-r/opb/rep/r-rep-f.2106-1-2010-pdf-e.pdf
[25] International Telecommunication Union Radio Communication. (2012). *Propagation Data Required for the Design of Terrestrial Free-Space Optical Links*. [Online]. Available: https://www.itu.int/rec/R-REC-P.1817/en
[26] International Telecommunication union radio communication. (2007). *Prediction Methods Required for the Design of Terrestrial Free-Space Optical Links*. [Online]. Available: https://www.itu.int/rec/R-REC-P.1814-0-200708-I/en
[27] Y. Furukawa and J. S. Wettlaufer, "Snow and ice crystals," *Phys. Today*, vol. 60, no. 12, pp. 70–71, Dec. 2007, doi: 10.1063/1.2825081.
[28] S. S. Joshil and V. Chandrasekar, "Attenuation correction in weather radars for snow," *IEEE Trans. Geosci. Remote Sens.*, vol. 61, 2023, Art. no. 5102114, doi: 10.1109/TGRS.2023.3254555.
[29] S. G. Warren, "Optical properties of snow," *Rev. Geophys.*, vol. 20, no. 1, pp. 67–89, Feb. 1982, doi: 10.1029/rg020i001p00067.
[30] K. Chance and R. V. Martin, "Atmospheric scattering," in *Spectroscopy and Radiative Transfer of Planetary Atmospheres*. London, U.K.: Oxford Univ. Press, 2017, pp. 63–76, doi: 10.1093/oso/9780199662104.003.0007.
[31] The Norwegian Meteorological Institute and NRK. *Narvik Meteorological Station*. Accessed: May 20, 2023. [Online]. Available: https://www.yr.no/nb
[32] A. Belmonte and J. M. Kahn, "Capacity of coherent free-space optical links using diversity-combining techniques," *Opt. Exp.*, vol. 17, no. 15, pp. 12601–12611, Jul. 2009, doi: 10.1364/oe.17.012601.
[33] S. Song, Y. Liu, T. Xu, and L. Guo, "Hybrid FSO/RF system using intelligent power control and link switching," *IEEE Photon. Technol. Lett.*, vol. 33, no. 18, pp. 1018–1021, Sep. 2021, doi: 10.1109/LPT.2021.3076467.
[34] "Climate in Svalbard 2100—A knowledge base for climate adaptation," Norwegian Centre Climate Services (NCCS), Tech. Rep., 2019. [Online]. Available: https://klimaservicesenter.no/kss/rapporter/klima-pa-svalbard-2100
[35] "High latitude optical satellite communications—Cloud coverage in Norway," Norwegian Defense Res. Inst. (FFI), Tech. Rep., 2019. [Online]. Available: https://www.ffi.no/en/publications-archive/high-latitude-optical-satellite-communications-cloud-coverage-in-norway
[36] Ny-Ålesund Research Station. *Disable Wi-Fi and Bluetooth*. Accessed: Sep. 26, 2024. [Online]. Available: https://nyalesundresearch.no/disable-wi-fi-and-bluetooth/
[37] Northrop Grumman. *Arctic Satellite Broadband Mission*. Accessed: Sep. 16, 2024. [Online]. Available: https://www.northropgrumman.com/space/arctic-satellite-broadband-mission
[38] Telenor Norway. *Coverage Map*. Accessed: Sep. 20, 2024. [Online]. Available: https://www.telenor.no/dekning/#dekningskart

SAHIL NAZIR POTTOO (Graduate Student Member, IEEE) received the M.Tech. degree in electronics and communication engineering from I. K. Gujral Punjab Technical University, India, in 2020. He is currently pursuing the Ph.D. degree in electrical engineering with the UiT The Arctic University of Norway, Narvik, Norway. His research interests include free-space optical communication, non-terrestrial networks, and unmanned aerial vehicles. He received the Gold Medal during the M.Tech. degree.

PÅL GUNNAR ELLINGSEN received the M.S. degree in applied physics and the Ph.D. degree in physics (optics) from the Norwegian University of Science and Technology (NTNU), in 2010 and 2014, respectively.

He is currently an Associate Professor with the UiT The Arctic University of Norway. He is a part of several research projects related to remote sensing, satellite construction, space debris, and optical communication. His research interests include optics, polarimetry, spectroscopy, remote sensing, satellite technology, data management, and education.

TU DAC HO (Senior Member, IEEE) received the M.Sc. and Ph.D. degrees in wireless communications from Waseda University, Tokyo, Japan, in 2005 and 2011, respectively.

He has been an Associate Professor with the Department of Electrical Engineering, UiT The Arctic University of Norway, since 2019. He joined the Department of Information Security and Communication Technology, Norwegian University of Science and Technology (NTNU), in November 2023, while continuing his position with UiT. He was an Assistant Professor with Waseda University, from 2011 to 2012; a Postdoctoral Fellow with NTNU, from 2012 to 2014; and a Senior Researcher with SINTEF Norway, from 2014 to 2018. He has participated in and led several scientific projects funded by the Norwegian Research Council and EU Horizon, focusing on the use of ML/AI for next-generation wireless communications and networks (6G and B6G) and the applications of unmanned aerial vehicles (UAVs) in these systems. He has published more than 50 international peer-reviewed publications and book chapters. His research interests include communication protocols, sustainable IoT, and path planning and optimization for radio networks with the assistance of autonomous vehicles, such as drones/UAVs and HAPS. He has served as a Committee Member/a Reviewer for many journals of IEEE, Elsevier, Wiley, IET, IEICE, and AIAA; and flagship conferences, such as IEEE GLOBECOM, ICC, and WCNC. He is an Editorial Board Member of Modern Subsea Engineering and Technology.